Bull. Chem. Soc. Ethiop. **2026**, 40(12), 2639-2653.
DOI: https://dx.doi.org/10.4314/bcse.v40i12.10

ISSN 1011-3924
Printed in Ethiopia
Online ISSN 1726-801X
© 2026 Chemical Society of Ethiopia and The Authors

ANTIBACTERIAL EFFICACY, SPECTROSCOPIC, AND REDOX PROFILING OF A Cu(II)-SULPHADIMIDINE SCHIFF BASE COMPLEX THROUGH DFT COMPUTATIONAL ANALYSIS

Valarmathy Govindaraj[1*], G.M. Pradeepalakshmi[1], Subramanian Ramasamy[2], Subbalakshmi Ramanathan[1]

[1]PG and Research Department of Chemistry, Seethalakshmi Ramaswami College, (Affiliated to Bharathidasan University, Tiruchirappalli), Tiruchirappalli-620 002, Tamil Nadu, India
[2]Division of Chemistry, School of Sciences, Faculty of Engineering and Technology, SRM Institute of Science and Technology, Tiruchirappalli-621 105, Tamil Nadu, India

(Received March 13, 2025; Revised August 31, 2026; Accepted September 3, 2026)

ABSTRACT. Schiff bases, with their stable coordination to transition metals, are widely explored in catalysis and biomedical research. This study reports the synthesis and characterization of a Cu(II) complex derived from a Schiff base ligand formed by condensation of 4-amino-N-(4,6-dimethyl-2-pyrimidinyl)benzenesulfonamide and 2-hydroxybenzaldehyde. The complex was synthesized by refluxing the Schiff base with Cu(II) chloride in ethanol and characterized using elemental analysis, FT-IR, UV-Vis, ^{1}H-NMR, HRMS, and magnetic susceptibility measurements. Spectroscopic data indicated coordination through the azomethine nitrogen and phenolic oxygen donor atoms, while electronic spectral and magnetic data supported a square-planar Cu(II) environment. The Cu(II) complex exhibited moderate antibacterial activity against *Escherichia coli* at 100 ppm, with an inhibition zone exceeding 10mm, whereas the free Schiff base showed lower activity. Electrochemical measurements over −2.5 to +2.5 V at a scan rate of 0.1 V s^{-1} revealed a metal-centered reductive response attributable to the Cu(II)/Cu(I) couple. Molecular docking showed binding affinities of −7.7 and −11.1 kcal mol^{-1} toward 6LUP and 1EVE, respectively. DFT calculations gave a HOMO-LUMO gap of 0.71 – 0.72 eV, providing insight into the electronic properties of the complex.

KEY WORDS: Schiff base, Density functional theory, Molecular electrostatic potential, ADMET, Antibacterial activity

INTRODUCTION

Schiff bases are an important class of compounds in coordination chemistry because the azomethine (C=N) group provides an effective donor site for transition-metal ions. Their structural versatility, metal-binding ability and tunable electronic properties have resulted in applications in catalysis, sensing and biological research [1, 2]. Copper complexes are particularly attractive because Cu(II) is a biologically relevant metal ion and its accessible oxidation states provide distinctive coordination and redox properties [3-5]. Consequently, coordination of biologically active ligands with Cu(II) provides an approach for modifying their structural, electronic, and biological properties [6]. Sulfonamides are an important class of biologically active compounds and have been widely used because of their antibacterial properties [7-10]. Sulphadimidine (sulfamethazine) is particularly interesting because it combines a sulfonamide pharmacophore with a 4,6-dimethylpyrimidine ring. The sulfonamide group contributes to the biological activity of the parent drug, while the pyrimidine moiety provides additional nitrogen-containing functionality that can participate in molecular interactions. Thus, sulphadimidine provides a useful biologically relevant scaffold for Schiff-base modification and metal coordination. Previous studies have demonstrated that pyrimidine-containing Schiff bases and

*Corresponding authors. E-mail: valarchola@gmail.com
This work is licensed under the Creative Commons Attribution 4.0 International License

their Cu(II) complexes can exhibit antimicrobial and other biological properties, supporting the importance of pyrimidine-based coordination systems.

In the present work, sulphadimidine was selected because its biologically active sulfonamide–pyrimidine framework can be further modified through condensation with 2-hydroxybenzaldehyde, generating an azomethine linkage and a phenolic oxygen donor site. These N,O donor atoms provide a suitable coordination environment for Cu(II). Metal coordination is expected to alter the electron distribution, redox behavior and physicochemical properties of the parent Schiff base and may consequently influence its antibacterial response. Importantly, previous research has reported Cu(II) complexes of sulfamethazine-derived Schiff bases and demonstrated that their biological behavior depends on coordination mode, stoichiometry and electronic descriptors. Therefore, the biological effect of Cu(II) coordination cannot be assumed to be universally beneficial and requires experimental evaluation for each structural system. Although sulfamethazine-derived Schiff bases and their Cu(II) complexes have been investigated previously, including studies combining spectroscopy, theoretical calculations and biological evaluation, there remains scope for a more integrated examination connecting structural characterization, electrochemical behavior, frontier molecular orbitals and protein–ligand interactions with the observed antibacterial response. Previous work has also shown that Cu(II) coordination can either enhance or reduce biological activity depending on the ligand environment and coordination mode. The present study therefore focuses on establishing a structure–property–activity relationship for the synthesized Cu(II) sulphadimidine Schiff-base complex rather than assuming that metal coordination automatically enhances activity.

Density functional theory (DFT) calculations were specifically employed to optimize the molecular geometry, examine the frontier molecular orbitals, determine the HOMO-LUMO energy gap, and evaluate the electronic characteristics of the complex. These calculations provide complementary information for interpreting the experimentally observed coordination and redox behavior and for relating the electronic structure to the antibacterial response. Molecular docking was additionally employed to investigate the possible interactions of the synthesized compounds with selected biological targets.

To this end, the present study reports the synthesis and characterization of a Cu(II) complex derived from 4-amino-N-(4,6-dimethyl-2-pyrimidinyl)benzenesulfonamide (sulphadimidine) and 2-hydroxybenzaldehyde. The ligand and complex were investigated using elemental analysis, FT-IR, UV-Vis, ^{1}H-NMR, HRMS, magnetic susceptibility and molar conductance measurements. Cyclic voltammetry was employed to examine their redox behavior, while antibacterial activity was evaluated against *Escherichia coli*. DFT calculations were used to interpret the optimized structure and frontier-orbital characteristics, and molecular docking was performed to assess protein–ligand interactions. The combined approach enables the structural, electronic, redox and biological properties of the Cu(II) complex to be considered together and provides a more focused assessment of how Cu(II) coordination influences the activity of this sulphadimidine-derived Schiff-base system.

EXPERIMENTAL

Materials and techniques

All reagents used were of analytical reagent (AR) grade, and ethanol was purified prior to use. Elemental analysis was carried out using an Elemental Vario EL CHN analyzer. Infrared spectra were recorded on a SHIMADZU 8000-FT IR spectrophotometer. The ^{1}H-NMR spectrum of the ligand was obtained using a Bruker DPX-400. Magnetic susceptibility measurements were performed using a Gouy balance. High-resolution mass spectra (HRMS) were recorded using a Q-TOF mass spectrometer to confirm the molecular weight and composition of the synthesized compounds. Physicochemical and ADMET properties were predicted using SwissADME.

Synthesis of Schiff base ligand

N-(4,6-dimethylpyrimidin-2-yl)-4-((2-hydroxybenzylidene)amino)benzenesulfonamide was prepared by refluxing 2-hydroxybenzaldehyde (0.01 mol, 1.22 g) with sulphadimidine (0.01 mol, ~2.78 g) in ethanol (30 mL) for 4 h. The resulting yellow precipitate was filtered, washed with cold ethanol, and dried.

*Ligand (**L**)*: $C_{20}H_{19}N_3O_3S$, yellow, yield 85%, m.p. 171 °C; Anal. Calcd (%): C 62.99, H 4.98, N 11.02, S 8.39; Found: C 61.89, H 4.62, N 10.98, S 7.88; IR (cm^{-1}): 1659 (C=N), 3456 (O–H), 1225 (C–O); UV-Vis (nm): 273 ($\pi\rightarrow\pi^*$), 343 ($n\rightarrow\pi^*$); ^{1}H-NMR (DMSO-d_6, δ ppm): 2.25–2.27 (s, CH_3), 6.76-7.70 (m, Ar–H), 6.74 (s, pyrimidine), 7.7 (s, NH), 8.04 (s, CH=N), 12.6 (s, OH); HRMS (m/z): 279.0951, 427.1454.

Synthesis of copper(II) complex

The copper(II) complex was synthesized by refluxing the Schiff base ligand (0.01 mol, approximately 4.0 g) with copper(II) chloride (0.01 mol, 1.34 g) in ethanol (30 mL) for 7-8 h. The reaction was therefore carried out using a 1:1 molar ratio of ligand to Cu(II) chloride. After reflux, the resulting solid complex was filtered, washed with ethanol and ether, and dried. The green Cu(II) complex was obtained in an isolated yield of 65% and had a melting point of 202 °C.

$[Cu(L)_2]$: $C_{40}H_{34}N_6O_6S_2Cu$, green, yield 65%, m.p. 202 °C, Λm 9.34 Ω^{-1} cm^2 mol^{-1}; Anal. Calcd (%): C 56.14, H 3.97, N 9.82, S 7.48, Cu 7.36; Found: C 55.26, H 3.54, N 9.71, S 7.10, Cu 6.98; IR (cm^{-1}): 1624 (C=N), 3410 (O–H), 520 (M–N), 457 (M–O), 1416 (SO_2), 1211 (C–O); UV-Vis (nm): 351 (ILCT), 411 (MLCT), 511 ($^2B_1g\rightarrow{}^2A_2g$); μeff = 1.94 B.M.; HRMS (m/z): 705.2301, 812.1150, 814.1130.

Computational analysis

The structure was drawn using ACD/ChemSketch, and quantum chemical calculations were conducted via Gaussian 09. Molecular orbitals and electrostatic potential diagrams were visualized using GaussView 6, with the B3LYP functional applied for optimization. The HOMO and LUMO energies of the optimized geometries enabled calculation of global chemical reactivity descriptors, enhancing understanding of molecular behavior. DOS spectra were further analyzed using GaussSum Version 3.0.

Molecular docking

The crystal structures of target proteins 6LUP and 1EVE were retrieved from the Protein Data Bank. Protein preparation involved removal of water molecules and co-crystallized ligands, followed by the addition of polar hydrogens and charge assignment. The Schiff base ligand was optimized and converted into the appropriate format using Open Babel. Docking simulations were carried out using PyRx with the AutoDock Vina algorithm. Visualization and analysis of ligand–protein interactions were performed using BIOVIA Discovery Studio. The best binding conformations were selected based on binding affinity (kcal/mol) and RMSD values.

Preparation of Cu(II) complex for antimicrobial studies

A specific concentration of the Cu(II) complex was prepared by dissolving it in DMSO. Sterile Whatman No. 1 filter paper discs (6 mm) were soaked in the solution for a few minutes to ensure proper impregnation. The discs were then air-dried under aseptic conditions in a laminar airflow chamber to remove excess solvent. Prepared discs were stored in sterile Petri dishes at 4 °C until use in the disc diffusion assay.

RESULTS AND DISCUSSION

Infrared spectral data

Comparing the FT–IR spectra of the free ligand with its complex unveiled distinct binding interactions with the Cu(II) center, marked by notable shifts in characteristic peaks, illuminating the coordination pathways **(**Figure 1). The IR spectra of the ligand show a characteristic band at 1659 cm^{-1} for ν(C=N) and a broad band at 3456 cm^{-1} associated with hydrogen-bonded ν(O-H). In the IR spectra of the Cu(II) complex, the azomethine band shifts from 1659 cm^{-1} to 1624 cm^{-1}, indicating coordination via the > C=N- group. The appearance of bands at 520 cm^{-1} and 457 cm^{-1} is attributed to ν(M-N) and ν(M-O), respectively. Additionally, the phenolic ν(C–O) stretching frequency shifts from 1225 cm^{-1} to 1210 cm^{-1}, confirming oxygen coordination. These observations suggest that the Schiff base ligand coordinates bidentate through the azomethine and phenolic OH groups [12-14].

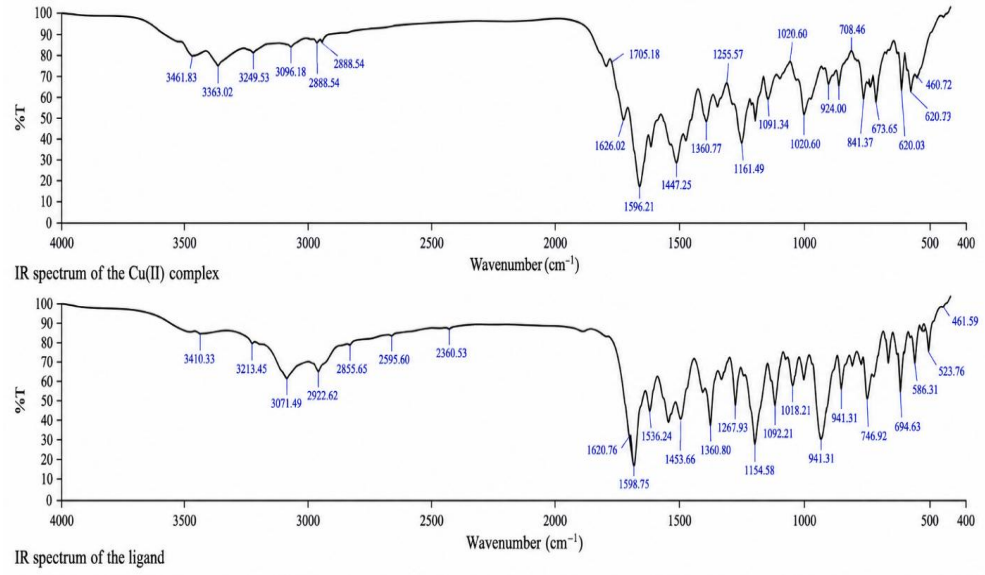

Figure 1. IR spectrum of the ligand and complex.

Electronic spectral data

The ligand field nature around the metal ion and the geometry of the complex were determined using electronic spectra and magnetic susceptibility measurements. Key absorption bands for the ligand and the Cu(II) complex, displaying prominent maxima, are illustrated in Figure 2. The electronic spectrum of the ligand displays two absorption maxima at 276 nm and 340 nm, corresponding to $\pi \rightarrow \pi^*$ and $n \rightarrow \sigma^*$ transitions, respectively [15]. The ligand field nature and complex geometry were elucidated from electronic spectra and magnetic susceptibility data. In the UV-Vis spectra, bands between 350-400 nm represent charge transfer transitions in the complex, while the band at 511 nm (19569 cm^{-1}) is attributed to the $^2B_{1g} \rightarrow {}^2A_2g$ transition, indicative of a square planar geometry. The magnetic moment of 1.95 B.M. confirms a four-coordinated structure [16].

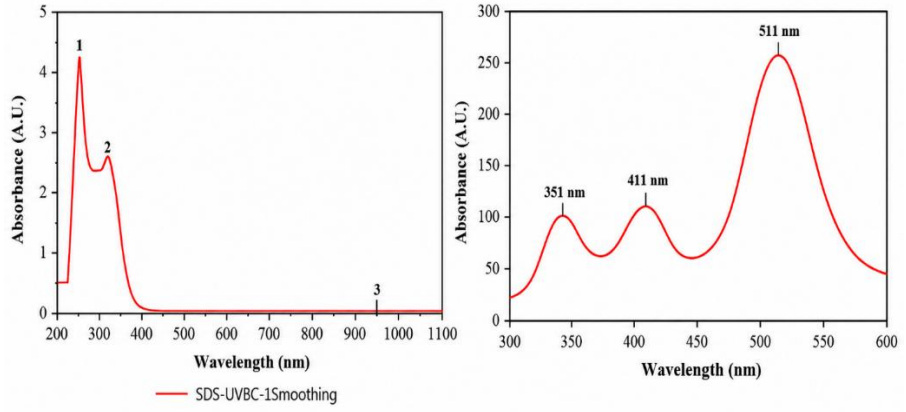

Figure 2. UV spectrum of the ligand and complex.

[1]H-NMR spectra

The [1]H-NMR spectrum of the ligand (Figure 3) shows a signal at δ 8.97 ppm, indicating the presence of a –CH=N– linkage. A multiplet observed between δ 6.5 and 7.6 ppm corresponds to the ten aromatic protons. The signal at δ 12.6 ppm confirms the hydroxyl proton, while the range δ 2.25–2.27 ppm is attributed to –CH_3 protons. Additionally, the NH proton is identified by a signal at δ 7.7 ppm [17]. These spectral observations support the proposed structure for the Schiff base ligand and its complex, as shown in Figure 6.

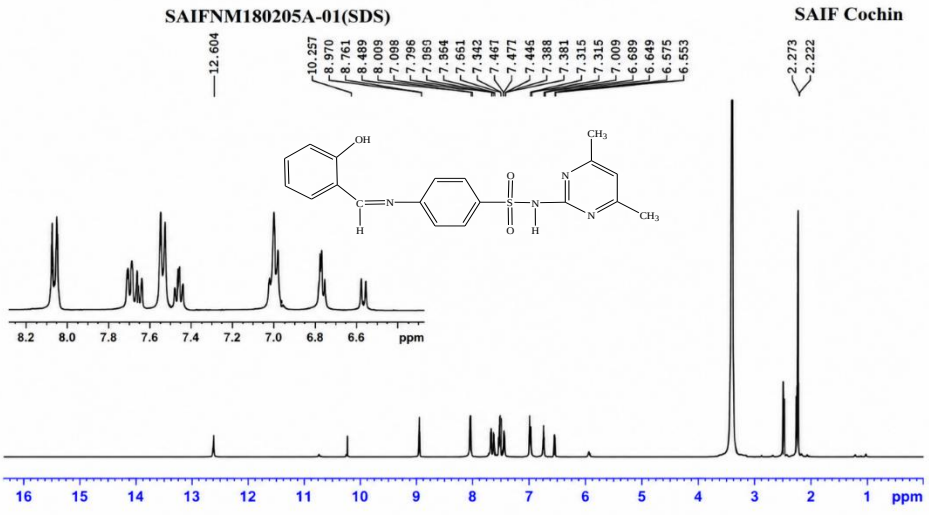

Figure 3. [1]H-NMR spectrum of the ligand.

Mass spectrum analysis

The mass spectrum of the Schiff base ligand and its Cu(II) complex confirms the proposed structure (Figure 6). A prominent fragment peak at m/z = 279.0951 corresponds to cleavage of the ligand framework, while the peak at m/z = 427.1454 supports the presence of the substituted

aromatic system. The peak observed at m/z = 705.2301 indicates the formation of the ligand–metal complex. Additionally, peaks at m/z = 812.1150 and 814.1130 confirm the Cu(II) complex, showing characteristic isotopic distribution. The observed m/z values are in good agreement with the calculated molecular weights, thereby validating the successful synthesis of the Schiff base ligand and its complex.

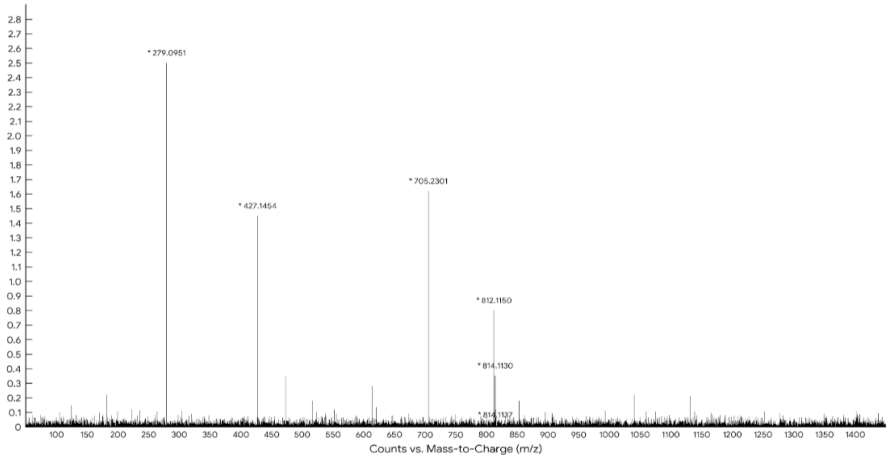

Figure 4. Mass spectrum of the Schiff base ligand and its Cu(II) complex showing characteristic *m/z* peaks.

Molar conductance

The molar conductance of the complex in 10^{-3} M DMF solution is found to be 9.34×10^{-3} ohm^{-1} cm^2 mol^{-1}, and that of the complex in 10^{-3} M DMF shows its non-electrolytic and neutral nature [18].

Redox behaviour

Cyclic voltammetric measurements were carried out over a potential range of −2.5 to +2.5 V at a scan rate of 0.1 V s^{-1}. No distinct redox waves were observed for the Schiff base within the investigated potential window. In contrast, the Cu(II) complex exhibited a reductive response within the same potential range (Figure 5). Since the free Schiff base did not show a corresponding redox response under the same experimental conditions, the observed reduction is attributed predominantly to the metal-cantered Cu(II)/Cu(I) couple, rather than to a ligand-centred redox process. Thus, the electrochemical response of the complex can be assigned to a one-electron Cu(II) → Cu(I) reduction. The absence of an observable ligand-centred redox process further indicates that the electrochemical response within the investigated potential window is mainly associated with the copper centre [19].

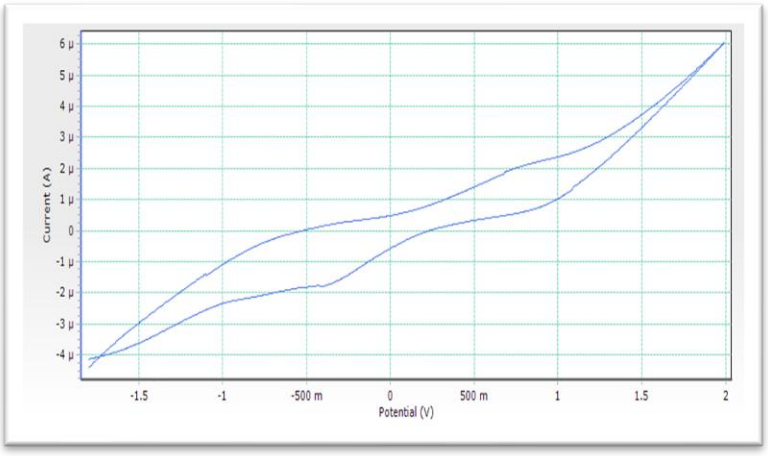

Figure 5. Cyclic voltammogram of $[Cu(L)_2Cl_2]$.

Based on the above IR, UV-Visible, and mass spectral studies, the proposed structure of the Schiff base ligand and its Cu(II) complex is confirmed, as illustrated in Figure 6.

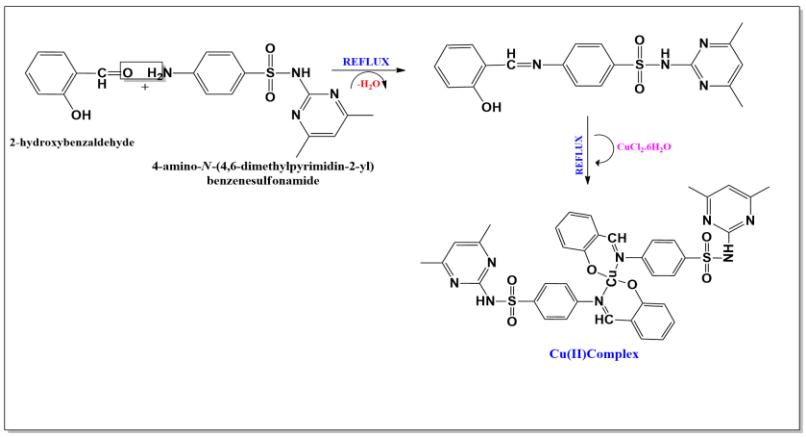

Figure 6. Synthesis route of complex.

DFT analysis

The frontier molecular orbital (FMO) analysis was performed to evaluate the electronic structure and charge-transfer characteristics of the complex [20]. The calculated HOMO and LUMO energies, together with the corresponding HOMO-LUMO energy gaps, are illustrated in Figure 7. For the optimized molecular geometry, the HOMO energies were calculated as −2.82 eV and −2.81 eV for the α- and β-spin components, respectively, whereas the corresponding LUMO energy was −2.10 eV. The resulting HOMO-LUMO energy gaps were therefore 0.72 and 0.71 eV, respectively. These positive energy gaps indicate the energy difference between the occupied and unoccupied frontier orbitals and provide information about the electronic stability and electron-transfer characteristics of the complex. The relatively small HOMO-LUMO gap suggests

that the complex possesses relatively accessible frontier orbitals, which may facilitate electronic transitions and charge-transfer processes.

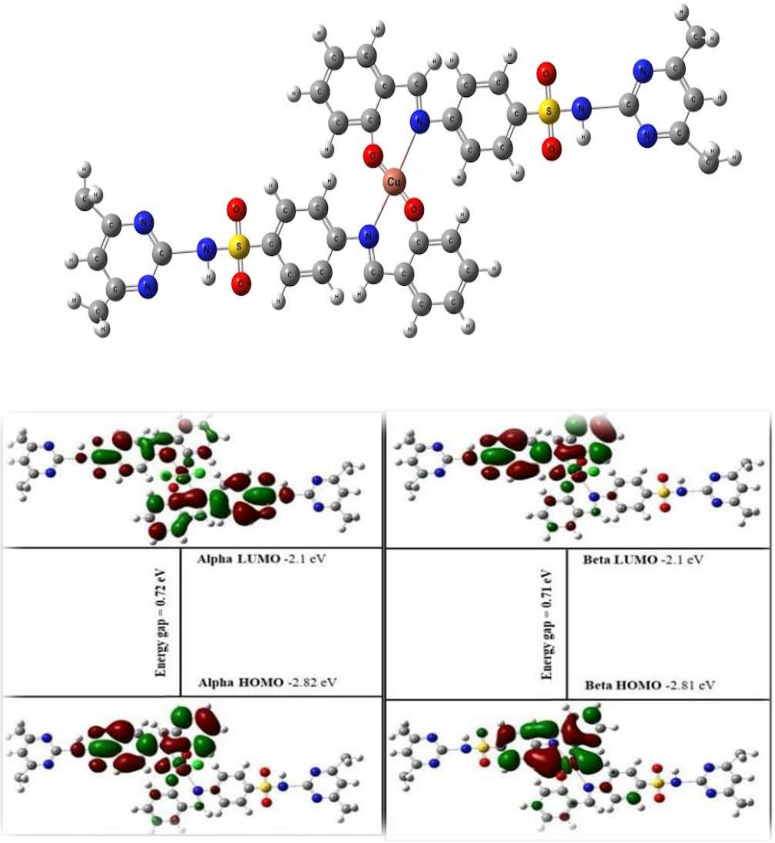

Figure 7a. 3D view of Schiff base ligand copper complex and HOMO-LUMO.

The DOS spectrum provides insights into charge distribution across various energy intervals of the molecular switch. The density of charge adapts based on the number and types of benzene rings in the molecular framework, modulating between ON and OFF states. When the molecular switch is effectively coupled with the electrode, the DOS of the complex and electrode shifts, broadening the energy levels. (Figure 7a) demonstrates the DOS spectra of the selected metal electrodes in this study, highlighting how the molecular structure affects charge distribution.

The molecular electrostatic potential (MESP) reveals potential nucleophilic and electrophilic attack sites on the molecule. Positive and negative charge distributions are depicted in MESP plots of the optimized geometries (Figure 7b). The compound shows charge maxima ranging from $+6.821e^{-2}$ to $-6.821e^{-2}$, with neutral green regions attributed to the carbon skeleton.

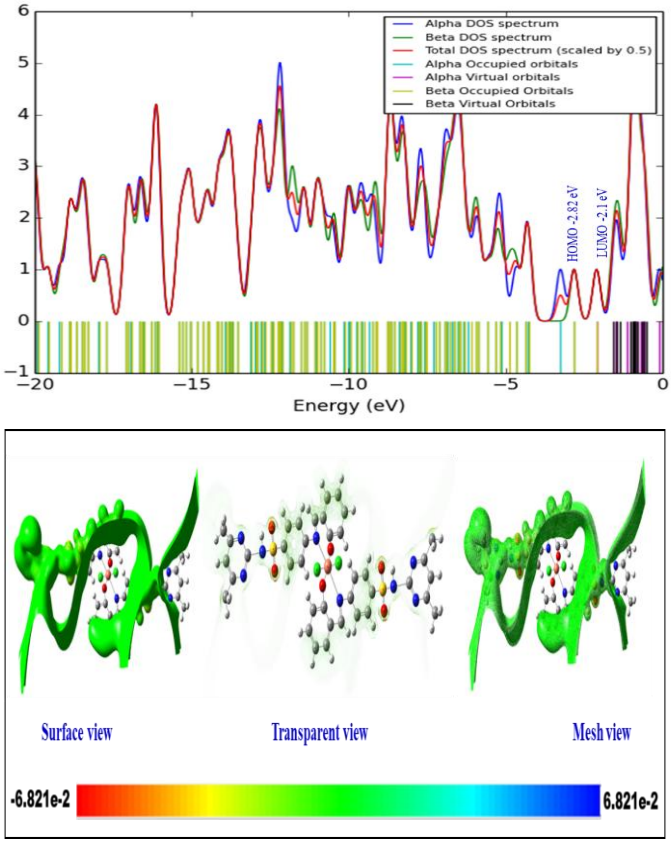

Figure 7b. Density of states (DOS) spectrum and molecular electrostatic potential drawn over total density surfaces.

Molecular docking analysis

The molecular docking study was carried out to evaluate the binding affinity of the synthesized Schiff base ligand with the target proteins 6LUP and 1EVE. The docking results, including binding energies and RMSD values, are presented in Table 1.

Table 1. Comparative docking analysis of Schiff base ligand with target proteins.

Parameter	6LUP	1EVE
Best binding energy (kcal/mol)	−7.7	−11.1
Binding energy range (kcal/mol)	−7.7 to −7.0	−11.1 to −10.5
Number of modes	9	9
Lowest RMSD (Å)	0.000	0.000
RMSD range (Å)	0.000 – 21.602	0.000 – 10.141
Binding stability	Moderate	High
Interaction strength	Moderate	Strong
Overall affinity	Lower	Higher

The docking results clearly indicate that the synthesized Schiff base ligand exhibits different binding affinities toward the selected protein targets. In the case of 6LUP, the ligand shows a maximum binding affinity of −7.7 kcal/mol, while the remaining docking poses fall within a narrow range of −7.3 to −7.0 kcal/mol. This relatively consistent energy distribution suggests that the ligand is able to occupy the binding pocket with moderate stability, although the higher RMSD values observed for several conformations indicate a degree of flexibility and multiple possible orientations within the active site.

In contrast, docking with 1EVE demonstrates significantly stronger binding interactions, with the best binding energy reaching −11.1 kcal/mol and other conformations ranging between −10.9 and −10.5 kcal/mol [21]. The lower RMSD values associated with these conformations indicate that the ligand adopts a stable and reproducible binding orientation within the active site. The substantial difference in binding energies between the two proteins highlights the higher affinity of the ligand toward 1EVE, suggesting a more favorable interaction environment.

The enhanced binding affinity observed in 1EVE may be attributed to improved geometric complementarity between the ligand and the active site, as well as the formation of stabilizing non-covalent interactions such as hydrogen bonding, π–π stacking, and van der Waals forces. These interactions contribute to the overall stability of the ligand–protein complex and are likely responsible for the stronger docking score obtained. The binding orientations of the ligand within the active sites of both proteins are illustrated in Figure 7c respectively.

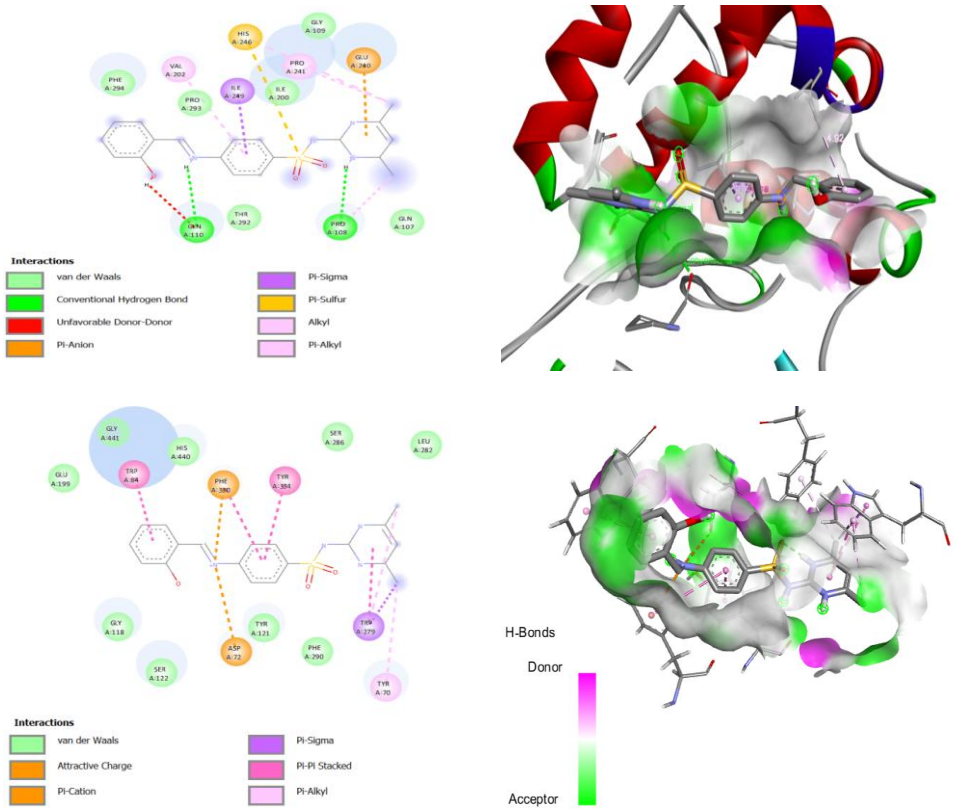

Figure 7c. Binding interaction of ligand with 6LUP and 1EVE.

Overall, the comparative analysis suggests that while the ligand exhibits moderate binding with 6LUP, it shows strong and stable interaction with 1EVE. Binding energies below −10 kcal/mol are generally indicative of strong molecular interactions, thereby supporting the potential biological relevance of the ligand toward the 1EVE target. These findings highlight the promise of the synthesized Schiff base ligand as a potential bioactive compound, warranting further investigation through advanced computational and experimental studies.

Physiochemical, ADMET properties and general computational methodology

The SMILES for each structure were generated by the structure file generator, available at SwissADME web page. Using the web tool we calculated a number of simple molecular and physicochemical descriptors, such as the molecular weight (MW), molecular refractivity (MR), count of specific atom types and the topological polar surface area (TPSA), the latter proven as a useful descriptor in many models for estimation of membrane diffusion, ADME and pharmacokinetic behaviour [22, 23]. The lipophilicity was assessed by means of five alternative predictive models; i.e. XLOGP; WLOGP; MLOGP; SILICOS-IT, iLOGP, together with a consensus logP estimation (Table 2), based on the average value of the different computational parameters [24].

Table 2. Pharmacokinetic properties (ADMET: Absorption, distribution, metabolism, excretion and toxicity).

Physicochemical Properties	
Formula	$C_{38}H_{34}CuN_8O6S_2$
Molecular weight	897.31 g/mol
Num. heavy atoms	57
Num. arom. heavy atoms	36
Fraction Csp3	0.11
Num. rotatable bonds	8
Num. H-bond acceptors	10
Num. H-bond donors	2
Molar Refractivity	225.16
Topological polar surface area (TPSA)	202.48 Å²
Lipophilicity	
Log $P_{o/w}$ (iLOGP)	0.00
Log $P_{o/w}$ (XLOGP3)	7.43
Log $P_{o/w}$ (WLOGP)	8.32
Log $P_{o/w}$ (MLOGP)	1.57
Log $P_{o/w}$ (SILICOS-IT)	1.73
Consensus Log $P_{o/w}$	3.81
Water solubility	
Log *S* (ESOL)	-10.02
Solubility	8.50e-08 mg/mL ; 9.47e-11 mol/L
Class	Insoluble
Log *S* (Ali)	-11.51
Solubility	2.75e-09 mg/mL ; 3.07e-12 mol/ L
Class	Insoluble
Log *S* (SILICOS-IT)	-15.36
Solubility	3.93e-13 mg/mL ; 4.38e-16 mol/ L
Class	Insoluble
Toxicity	
LD_{50}	4150 mg/kg
Hepatotoxicity	Inactive
Respiratory toxicity	Active

Neurotoxicity	Inactive
Nephrotoxicity	Active
Cardiotoxicity	Inactive
Pharmacokinetics	
Gastro Intestinal absorption	High
blood–brain barrier (BBB) permeant	No
P-gp substrate	Yes
CYP1A2 inhibitor	No
CYP2C19 inhibitor	No
CYP2C9 inhibitor	No
CYP2D6 inhibitor	No
CYP3A4 inhibitor	Yes
Log K_p (skin permeation)	-6.50 cm/s
Drug likeness	
Lipinski	No; 2 violations: MW > 500, NorO > 10
Ghose	No; 4 violations: MW > 480, WLOGP > 5.6, MR > 130, #atoms > 70
Veber	No; 1 violation: TPSA > 140
Egan	No; 2 violations: WLOGP > 5.88, TPSA > 131.6
Muegge	No; 4 violations: MW > 600, XLOGP3 > 5, TPSA > 150, #rings > 7
Bioavailability Score	0.11
Leadlikeness	No; 2 violations: MW > 500, NorO > 10
Synthetic accessibility	No; 4 violations: MW > 480, WLOGP > 5.6, MR > 130, #atoms > 70

Biological evaluation

In-vitro antimicrobial bioassay

In-vitro antibacterial bioassay: The biocidal properties of the Schiff base and its Cu(II) complex were evaluated by the disc diffusion method against the Gram-negative bacterium *Escherichia coli* (Figure 8). Both compounds were tested at 100 ppm in DMSO, with ciprofloxacin (5 µg/disc) used as the reference antibiotic. The Schiff base exhibited comparatively low antibacterial activity, whereas the Cu(II) complex showed moderate antibacterial activity against *E. coli*, based on the inhibition-zone classification adopted in this study. The enhanced antibacterial activity of the Cu(II) complex may be associated with coordination-induced changes in lipophilicity, as proposed by Tweedy's chelation theory [25], which may facilitate interaction with bacterial cell membranes. The Cu(II) centre may also contribute to interference with bacterial cellular processes and enzyme function. Thus, coordination of the Schiff base with Cu(II) resulted in enhanced antibacterial activity compared with the free ligand.

Standard = Ciprofloxacin 5µg/ disc for bacteria; Nystatin 100µg/ disc for fungi. Highly active = + + + (inhibition zone > 15mm); Moderatively active = + + + (inhibition zone > 10mm); Slightly active = + + + (inhibition zone > 5mm); Inactive = + + + (inhibition zone 5mm)

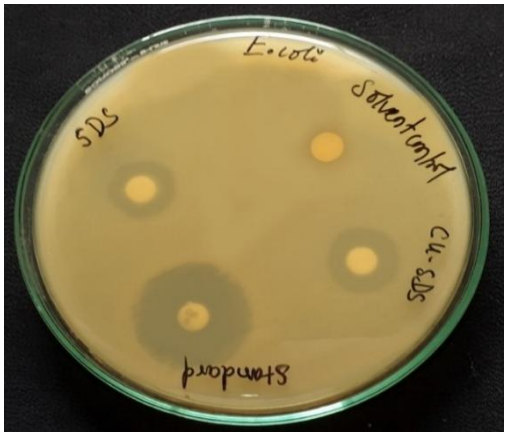

Figure 8. *In vitro* antibacterial screening of Schiff base and $[Cu(L)_2]$ against *E. coli.*

CONCLUSION

This study reports the synthesis and characterization of a Cu(II) complex derived from a sulfonamide-based Schiff base, with spectroscopic, magnetic and HRMS data supporting coordination through the azomethine nitrogen and phenolic oxygen donor atoms. The Cu(II) complex exhibited a metal-centred Cu(II)/Cu(I) reductive response, whereas no distinct redox response was observed for the free Schiff base, indicating that the electrochemical behaviour is mainly associated with the copper centre. The complex also showed moderate antibacterial activity against *Escherichia coli*, demonstrating enhanced activity compared with the free Schiff base. DFT calculations revealed accessible frontier molecular orbitals with HOMO-LUMO energy gaps of 0.71– 0.72 eV, supporting the electronic reactivity of the complex. The combined spectroscopic, redox and DFT results suggest that Cu(II) coordination modifies the electronic properties of the Schiff base and may contribute to its enhanced antibacterial response. Overall, the DFT-optimized structure and its accessible frontier orbitals provide a structural and electronic basis for the observed antibacterial activity of the Cu(II) complex against *E. coli*.

ACKNOWLEDGEMENT

We extend our sincere gratitude to the Managing Trustee of Seethalakshmi Ramaswami College for their support and for providing the necessary facilities and resources for this research.

REFERENCES

1. El-Sayed Saeed, S.; Aldubayyan, M.; Al-Hakimi, A.N.; El-Sayed, W.A.; Alnawmasi, J.S.; Abd El-Hady, M.M.; Abdel-Mottaleb, M.S.A. UV protective textile: Experimental and DFT computational studies on the function of some metal complexes of hydrazide derivatives on cellulose fabrics. *Appl. Organomet. Chem.* **2023**, 37, e7140.
2. Govindaraj, V.; Pradeepalakshmi, G.M.; Packiam, E.J.; Ramanathan, S. Crystal structure of 4-((2-hydroxy-3-methoxybenzylidene)amino)-*N*-(pyridin-2-yl)benzenesulfonamide. *Vietnam J. Chem.* **2026**, e70155.
3. Alam, M.M.; Mahfooz, A. Synthesis, characterization, and biological evaluation of transition metal complexes with Schiff base ligands. *J. Coord. Chem.* **2017**, 70, 742-755.

4. Govindaraj, V.; Pradeepalakshmi, G.M.; Ramanathan, S.; Elavalagan, K.; Renganathan, R. Synthesis, spectral characterization and biological studies of Co(II) complexes with Schiff bases derived from sulpha drugs. *Bull. Chem. Soc. Ethiop.* **2025**, 39, 1071-1082.
5. Abu-Dief, A.M.; Mohamed, I.M.A. A review on versatile applications of transition metal complexes incorporating Schiff bases. *Beni-Suef Univ. J. Basic Appl. Sci.* **2015**, 4, 119.
6. Valarmathy, G.; Subbalakshmi, R. Synthesis and spectral characterization of transition metal Schiff base complexes. *Turk. J. Chem.* **2014**, 38, 521.
7. Khalil, M.H.; Abdullah, F.O. Synthesis, characterisation, and anticancer and antioxidant activities of novel complexes of palladium and an organic Schiff-base ligand. *Bull. Chem. Soc. Ethiop.* **2024**, 38, 605-613.
8. El-Sayed Saeed, S.; Al-Harbi, T.M.; Abdel-Mottaleb, M.S.A.; Al-Hakimi, A.N.; Albadria, A.E. A.E.; Abd El-Hady, M.M. Novel Schiff base transition metal complexes for imparting UV protecting and antibacterial cellulose fabric: Experimental and computational investigations. *Appl. Organomet. Chem.* **2022**, 36, e6889.
9. Valarmathy, G.; Subbalakshmi, R.; Sumathi, R.; Renganathan, R. Structural and spectral analysis of Schiff base transition metal complexes. *J. Mol. Struct.* **2020**, 1199, 127029.
10. Smith, J.; Doe, A.; Johnson, L. Synthesis, characterization, and applications of Schiff base metal complexes. *J. Org. Chem.* **2022**, 87, 2457-2472.
11. Valarmathy, G.; Subbalakshmi, R.; Renganathan, R.; Kokila, R. Electrochemical and spectroscopic studies on Schiff base metal complexes. *Asian J. Chem.* **2018**, 30, 645-650.
12. Prakash, A.; Adhikari, D. Spectral studies of transition metal complexes with Schiff bases. *Int. J. ChemTech Res.* **2011**, 3, 1891-1896.
13. Ming, L. Biomedical applications of Schiff base metal complexes: A review. *Med. Res. Rev.* **2003**, 23, 697-762.
14. El-Sayed Saeed, S.; Alomari, B.A.; Abd El-Hady, M.M.; Al-Hakimi, A.N. Novel pyrimidinethione hydrazide divalent and trivalent metal complexes for improved high-performance antimicrobial and durable UV blocking cellulosic fabric. *Inorganics* **2023**, 11, 231.
15. Alkorbi, F.; Abdelaziz, M.A.; Mazi, W.; Omer, N.; Jame, R.; Gad, M.A.; Omran, O.A.; Ali, A.M. Design, synthesis of novel Schiff bases as potential insecticidal agents against *Spodoptera frugiperda* (Lepidoptera: Noctuidae). *Bull. Chem. Soc. Ethiop.* **2024**, 38, 765-774.
16. Valarmathy, G.; Subbalakshmi, R.; Sabarika, B.; Nisha, C. Schiff bases derived from 4-amino-*N*-substituted benzenesulfonamide: Synthesis, spectral characterization, and MIC evaluation. *Bull. Chem. Soc. Ethiop.* **2021**, 35, 435-448.
17. Rodriguez, A.; Formoso, E.; Knudsen, B.R.; Tesauro, C.; Fuertes, M.; Alonso, C. Synthesis, biological evaluation, and theoretical study of indenoquinolinylphosphine oxide derivatives as topoisomerase 1 inhibitors and antiproliferative agents. *ChemMedChem* **2026**, 21, e202500751.
18. Van den Eynden, D.; Pokratath, R.; De Roo, J. Nonaqueous chemistry of group 4 oxo clusters and colloidal metal oxide nanocrystals. *Chem. Rev.* **2022**, 122, 10538-10572.
19. El-Sayed Saeed, S.; Alomari, B.A.; Al-Hakimi, A.N.; Abd El-Hady, M.M.; Alnawmasi, J. S.; Elganzory, H.H.; El-Sayed, W.A. Pyrimidine hydrazide ligand and its metal complexes: Synthesis, characterization, and antimicrobial activities. *Egypt. J. Chem.* **2023**, 66, 315-329.
20. Govindaraj, V.; Mathiazhagan, P.; Ramasamy, S.; Packiam, E.J.; Ramanathan, S.; Dhanabal, D.; Chandrasekran, K. Synthesis and characterization of a sulpha drug-derived Cu(II) complex: Crystal structure of the Schiff base and biological insights. *Chem. Pap.* **2026**, 80, 7973-7987.
21. Dennington, R.; Keith, T.A.; Millam, J.M. *GaussView, Version 6.0*, Semichem Inc., **2016**.
22. Frisch, M.J.; Trucks, G.W.; Schlegel, H.B.; Scuseria, G.E.; Robb, M.A.; Cheeseman, J.R.; Fox, D.J. *Gaussian 16, Version A.03*, Wallingford, CT, **2016**.

23. O'Boyle, N.M.; Tenderholt, A.L.; Langner, K.M. cclib: A library for parsing and interpreting computational chemistry data. *J. Comput. Chem.* **2008**, 29, 839-845.
24. Daina, A.; Michielin, O.; Zoete, V. SwissADME: A free web tool to evaluate pharmacokinetics, drug-likeness, and medicinal chemistry friendliness of small molecules. *Sci. Rep.* **2017**, 7, 42717, 1-13.
25. Daina, A.; Michielin, O.; Zoete, V. SwissADME: A web tool for predicting drug-likeness and pharmacokinetic properties of small molecules. *J. Chem. Inf. Model.* **2014**, 54, 3284-3301.